Supplement of

An analysis coordinate transform to facilitate use of in-situ aircraft observations for flux estimations

Ariana L. Tribby and Paul O. Wennberg

Correspondence to: Ariana L. Tribby (aaalt02013@gmail.com) or Paul O. Wennberg (wennberg@caltech.edu)

Supplemental Information

S1 GEOS-Chem simulations during ATom winter 2017 Atlantic Ocean transect

Figure S1. GEOS-Chem-simulated C_2H_6 (ppb) Atlantic Ocean transect along pressure and latitude. Simulations were conducted for the ATom winter 2017 campaign time-period. A representative simulation transect was selected by slicing along a longitude of -30.0 degrees W and a single time point during the day shown in the column label. (We used the average longitude encountered along the Atlantic flight track. Latitude was not interpolated to exactly match the aircraft flight path in this figure.) Horizontal resolutions of 4 x 5 and 2 x 2.5 were interpolated along latitude and pressure to 0.5 x 0.625 resolution. The bottom panel is a zoomed-in illustration of row: 3, column: 2, with the aircraft flight path represented by the grey line, the aircraft observations shown in triangle markers and potential temperature contours shown in the black lines.

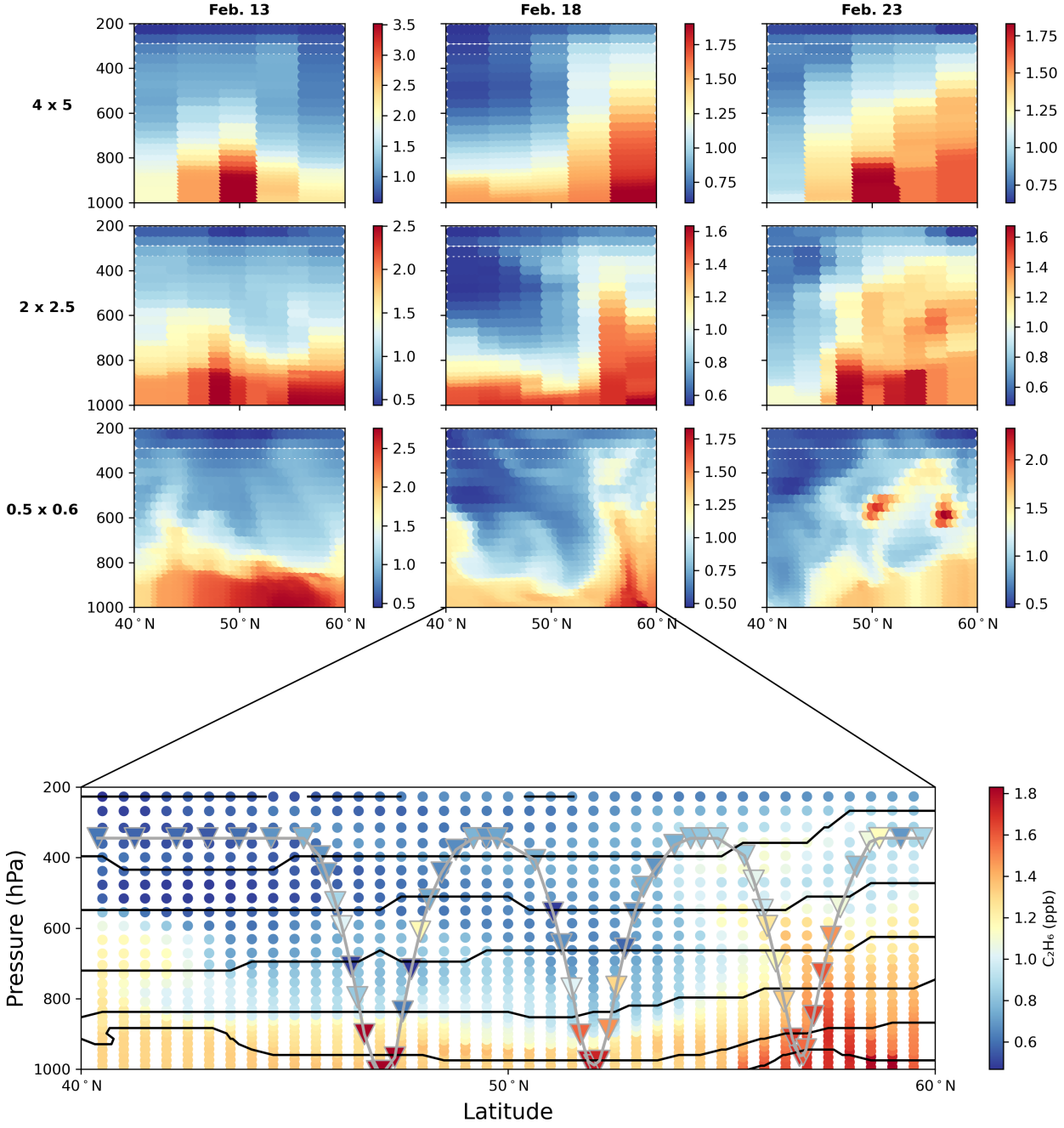

Figure S2. GEOS-Chem-simulated C_2H_6 (ppb) Atlantic Ocean transect along potential temperature and latitude. Simulations were conducted for the ATom winter 2017 campaign time-period. A representative simulation transect was selected by slicing along a longitude of -30.0 degrees W and a single time point during the day shown in the column label. (We used the average longitude encountered along the Atlantic flight track. Latitude was not interpolated to exactly match the aircraft flight path in this figure.) Horizontal resolutions of 4 x 5 and 2 x 2.5 were interpolated along latitude and pressure to 0.5 x 0.625 resolution. The bottom panel is a zoomed-in illustration of row: 3, column: 2, with the aircraft flight path represented by the grey line and the aircraft observations shown in triangle markers.

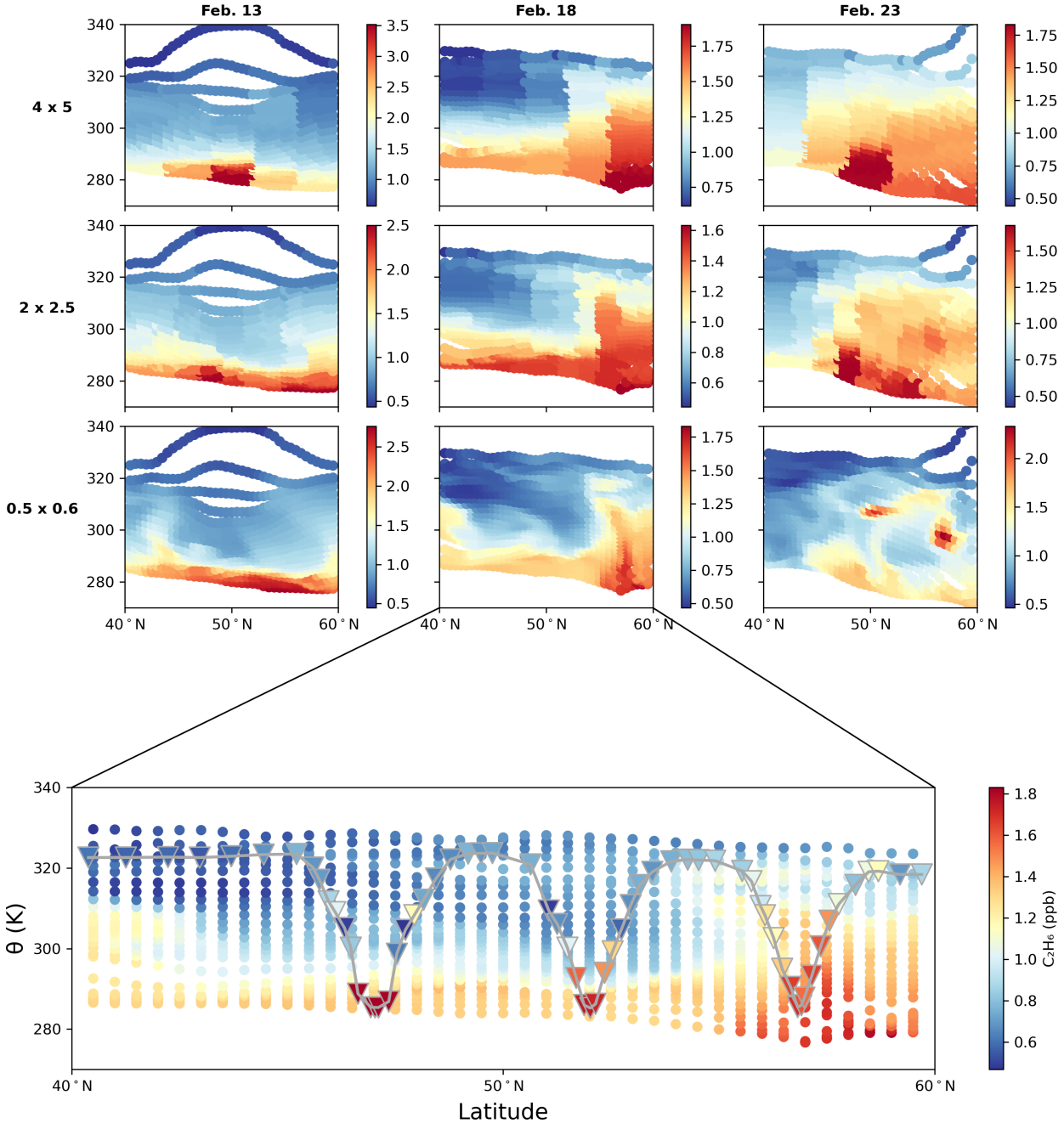

Figure S3. C_2H_6 vs potential temperature. GEOS-Chem simulations were conducted for the ATom winter 2017 time-period and were interpolated along aircraft flight path latitude, longitude, time and potential temperature. Feb 15-19th is the observed aircraft flight path time, and the left and right plots show times not actually observed by the aircraft and instead are GEOS-Chem simulations sampled 5 days before/after the plane start time.

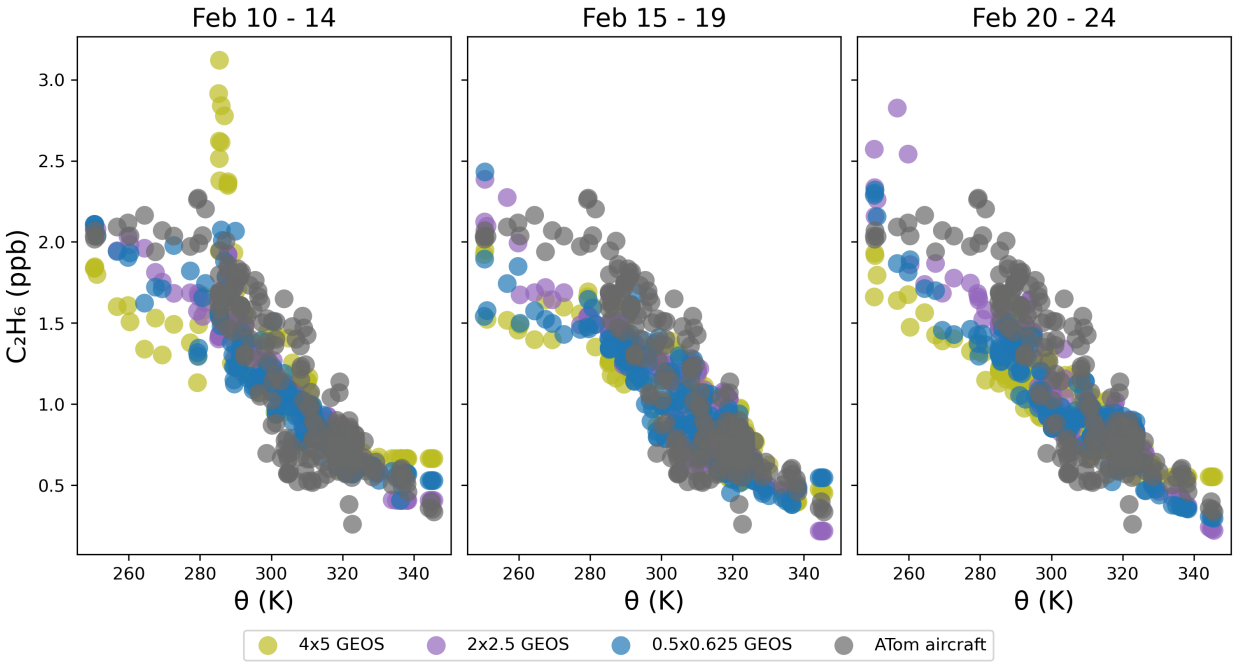

S2 GEOS-Chem simulations during ATom summer 2016 Atlantic Ocean transect

Elevated mole fractions of C_3H_8 and C_2H_6 in Figures S4 – S9 were not found to be a result of biomass burning using HCN and CO as tracers.

Figure S4. GEOS-Chem-simulated C_3H_8 (ppb) Atlantic Ocean transect along pressure and latitude. Simulations were conducted for the ATom summer 2016 campaign time-period. A representative simulation transect was selected by slicing along a longitude of -30.0 degrees W and a single time point during the day shown in the column label. (We used the average longitude encountered along the Atlantic flight track. Latitude was not interpolated to exactly match the aircraft flight path in this figure.) Horizontal resolutions of 4 x 5 and 2 x 2.5 were interpolated along latitude and pressure to 0.5 x 0.625 resolution. The bottom panel is a zoomed-in illustration of row: 3, column: 2, with the aircraft flight path represented by the grey line, the aircraft observations shown in triangle markers and potential temperature contours shown in the black lines.

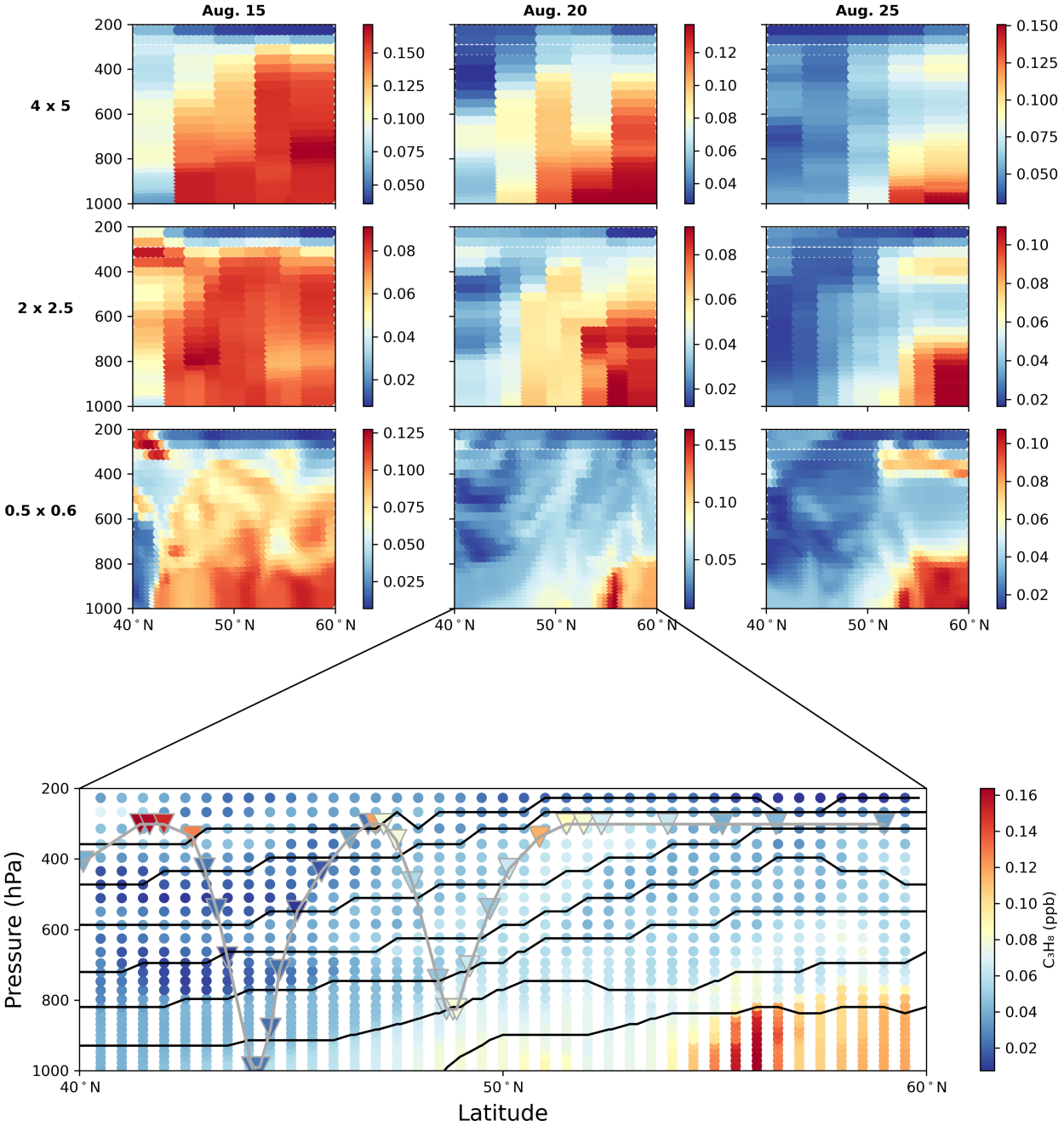

Figure S5. GEOS-Chem-simulated C_2H_6 (ppb) Atlantic Ocean transect along pressure and latitude. Simulations were conducted for the ATom summer 2016 campaign time-period. A representative simulation transect was selected by slicing along a longitude of -30.0 degrees W and a single time point during the day shown in the column label. (We used the average longitude encountered along the Atlantic flight track. Latitude was not interpolated to exactly match the aircraft flight path in this figure.) Horizontal resolutions of 4 x 5 and 2 x 2.5 were interpolated along latitude and pressure to 0.5 x 0.625 resolution. The bottom panel is a zoomed-in illustration of row: 3, column: 2, with the aircraft flight path represented by the grey line, the aircraft observations shown in triangle markers and potential temperature contours shown in the black lines.

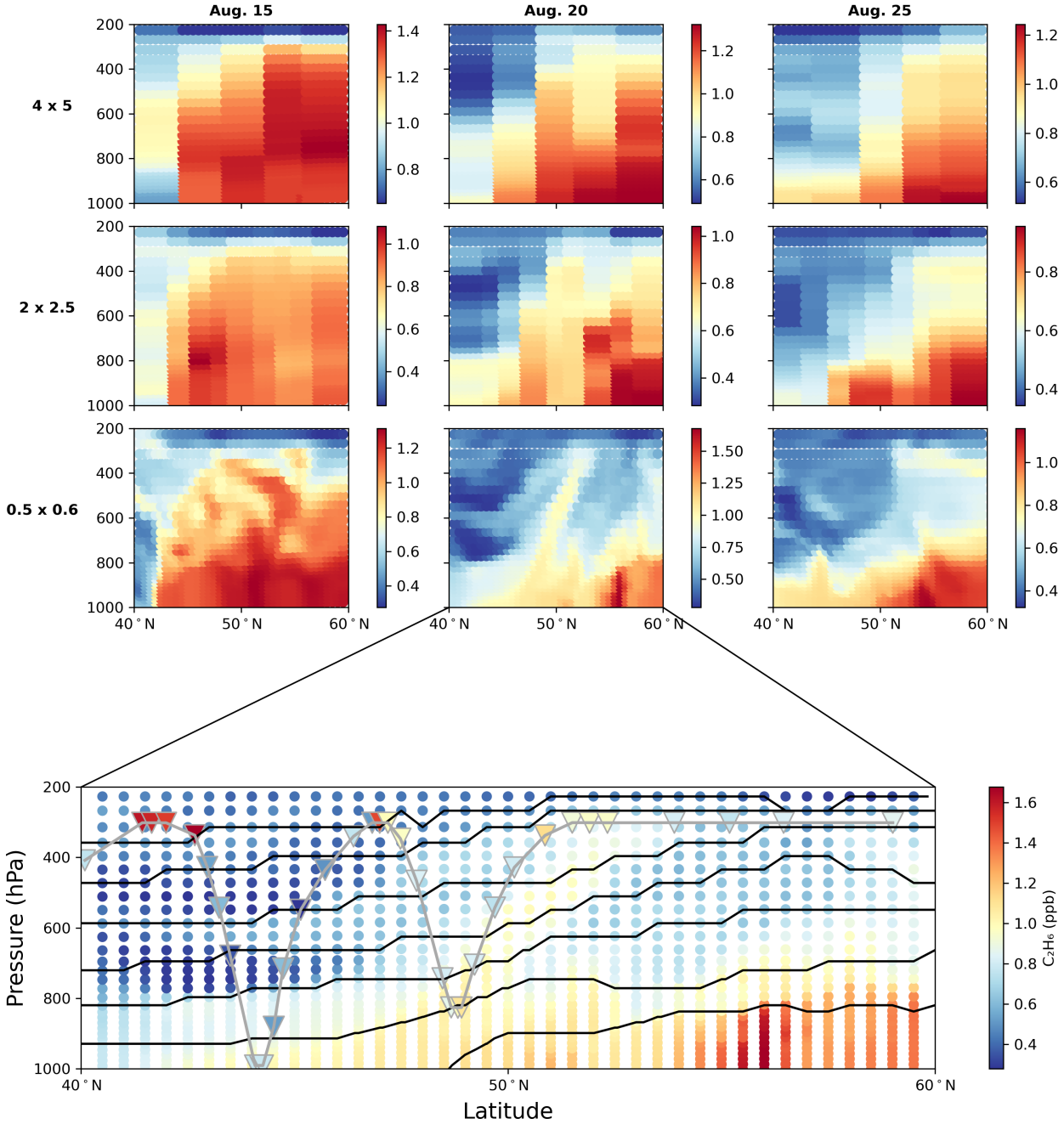

Figure S6. GEOS-Chem-simulated C_3H_8 (ppb) Atlantic Ocean transect along potential temperature and latitude. Simulations were conducted for the ATom summer 2016 campaign time-period. A representative simulation transect was selected by slicing along a longitude of -30.0 degrees W and a single time point during the day shown in the column label. (We used the average longitude encountered along the Atlantic flight track. Latitude was not interpolated to exactly match the aircraft flight path in this figure.) Horizontal resolutions of 4 x 5 and 2 x 2.5 were interpolated along latitude and pressure to 0.5 x 0.625 resolution. The bottom panel is a zoomed-in illustration of row: 3, column: 2, with the aircraft flight path represented by the grey line and the aircraft observations shown in triangle markers.

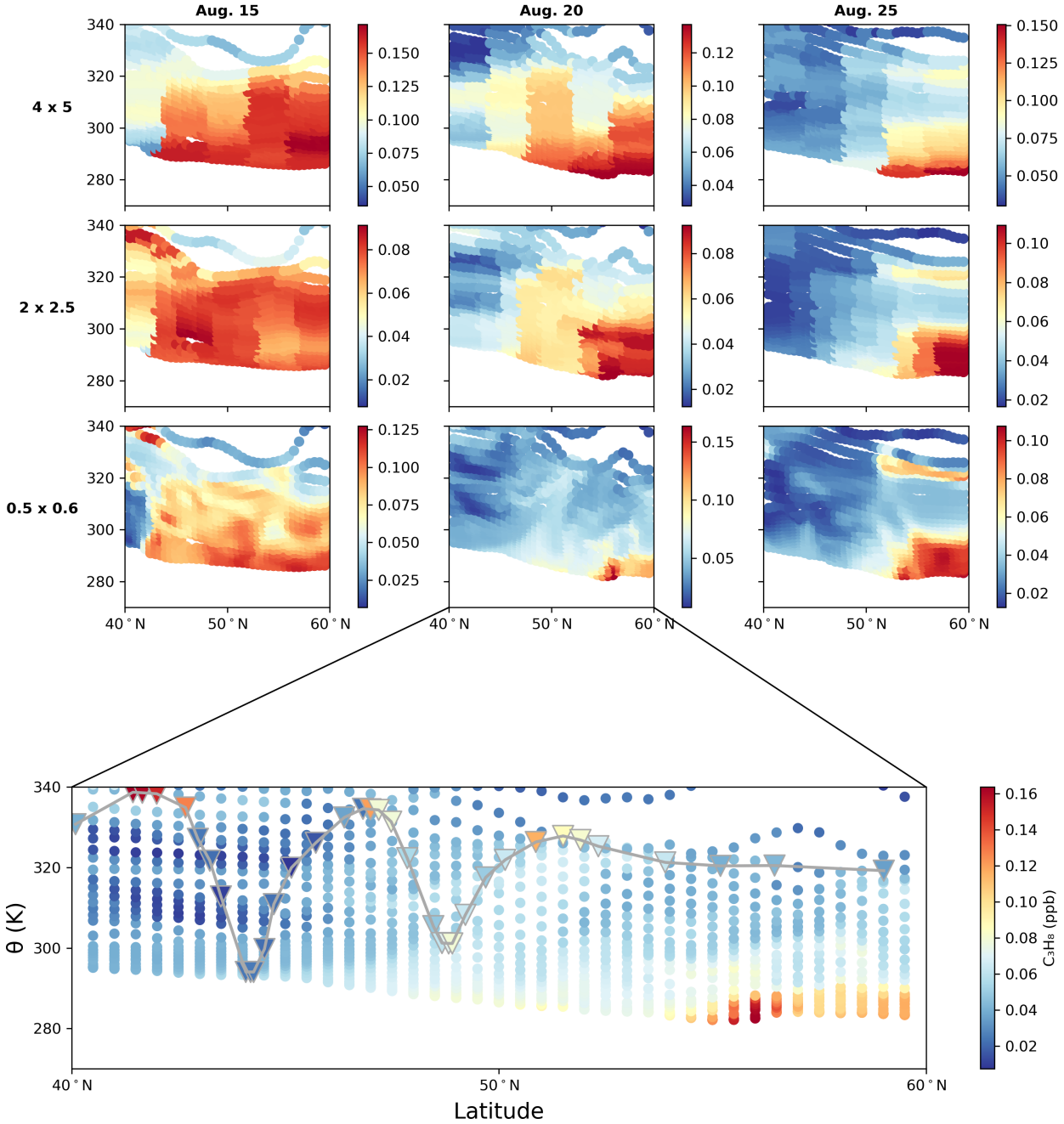

Figure S7. GEOS-Chem-simulated C_2H_6 (ppb) Atlantic Ocean transect along potential temperature and latitude. Simulations were conducted for the ATom summer 2016 campaign time-period. A representative simulation transect was selected by slicing along a longitude of -30.0 degrees W and a single time point during the day shown in the column label. (We used the average longitude encountered along the Atlantic flight track. Latitude was not interpolated to exactly match the aircraft flight path in this figure.) Horizontal resolutions of 4 x 5 and 2 x 2.5 were interpolated along latitude and pressure to 0.5 x 0.625 resolution. The bottom panel is a zoomed-in illustration of row: 3, column: 2, with the aircraft flight path represented by the grey line and the aircraft observations shown in triangle markers.

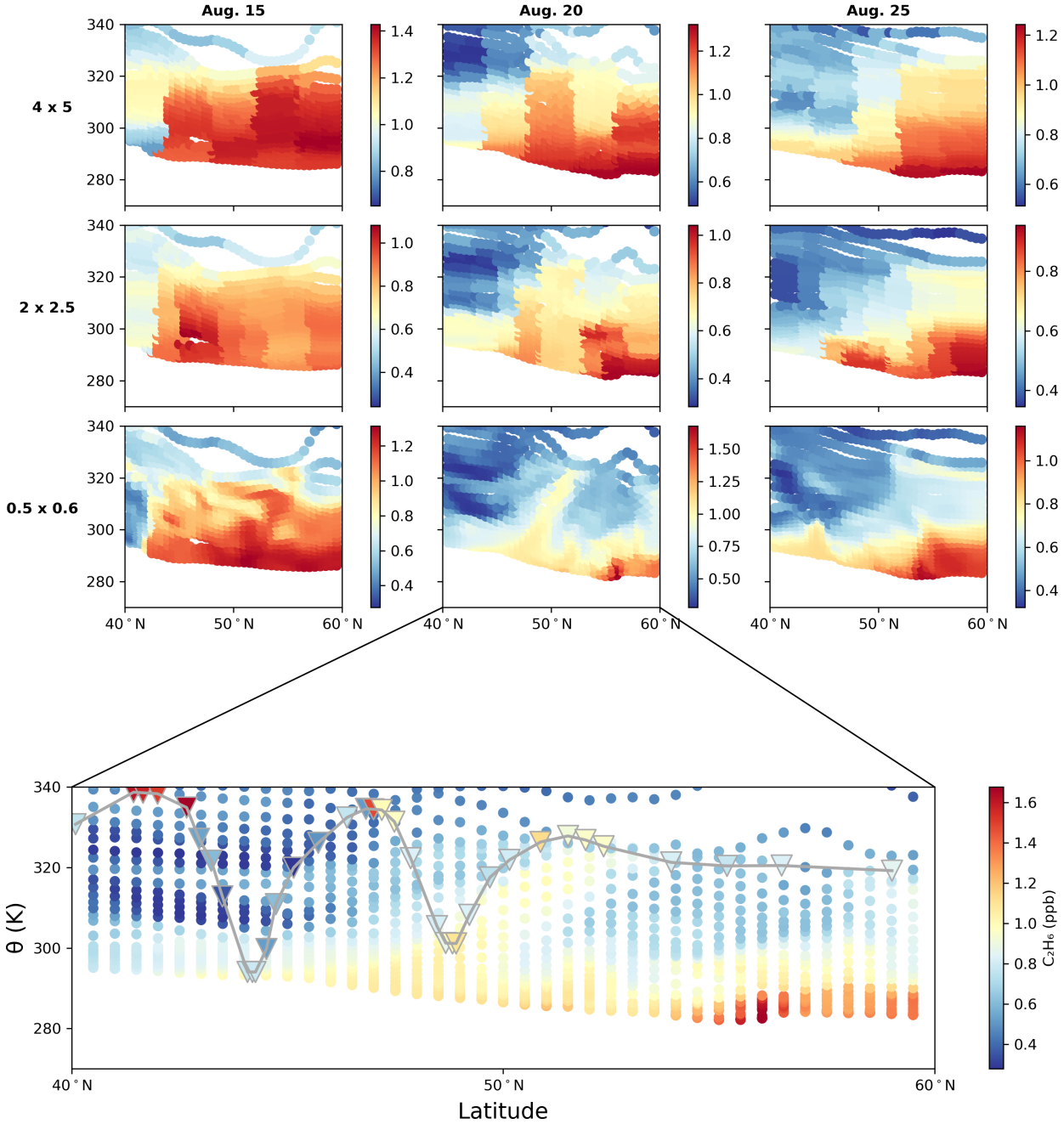

Figure S8. C_3H_8 vs potential temperature. GEOS-Chem simulations were conducted for the ATom summer 2016 campaign time-period and were interpolated along aircraft flight path latitude, longitude, time and potential temperature. Aug. 17-20th is the observed aircraft flight time, and the left and right plots show times not actually observed by the aircraft and instead are GEOS-Chem simulations sampled 5 days before/after the plane start time.

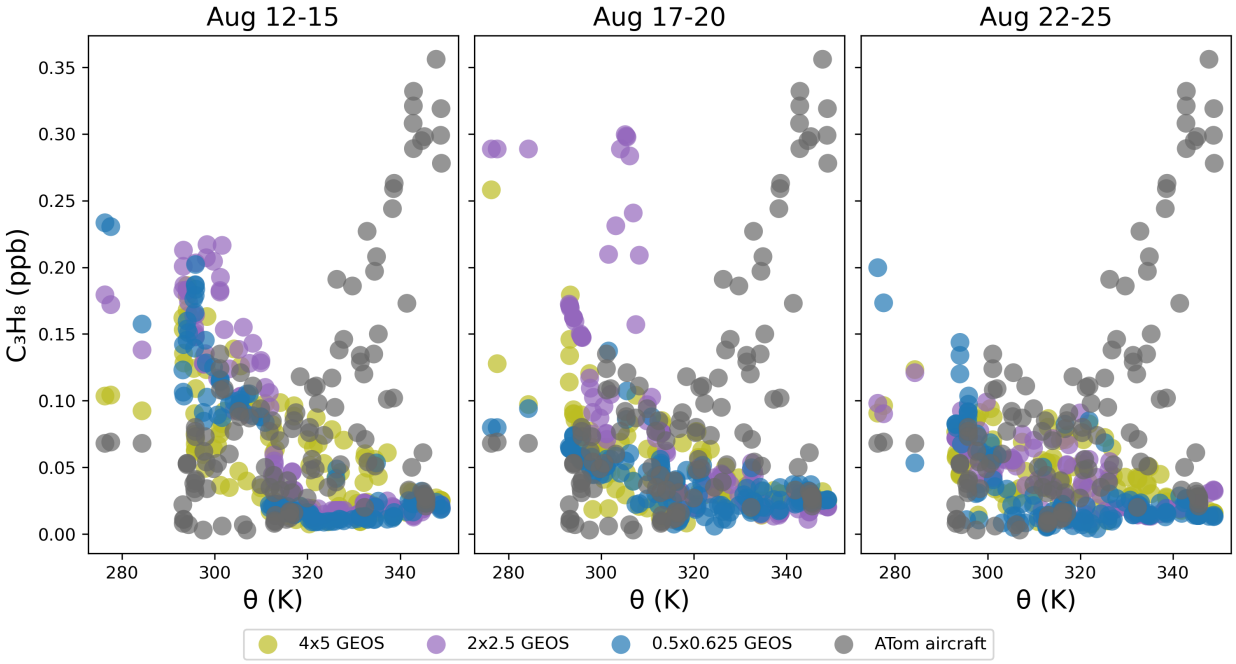

Figure S9. C_2H_6 vs potential temperature. GEOS-Chem simulations were conducted for the ATom summer 2016 campaign time-period and were interpolated along aircraft flight path latitude, longitude, time and potential temperature. Aug. 17-20th is the observed aircraft flight time, and the left and right plots show times not actually observed by the aircraft and instead are GEOS-Chem simulations sampled 5 days before/after the plane start time.

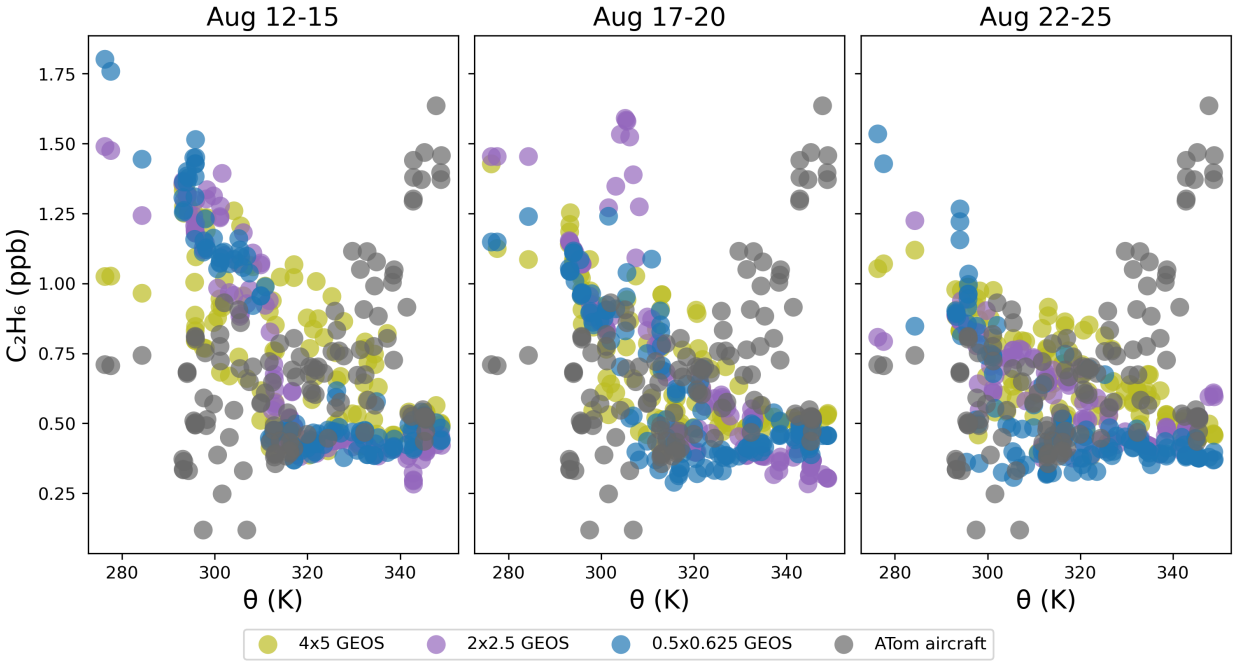

S3 Bayesian inference using simulations conducted for ATom winter 2017 Atlantic Ocean transect

We run our statistical model using Stan software version 2.26, (2021b) with CmdStanPy Python interface version 0.9.67, (2021a). We parse Markov chain sampling using ArviZ version 0.11.1, (Kumar et al., 2019). We validate our hierarchical model using simulation-based calibration, (Talts et al., 2020) and posterior predictive checks (described more below). We use bebi103 package version 0.1.0 (Bois, 2020a) to execute simulation-based calibration, prepare data for Stan sampling, parse MCMC samples, plot posteriors and plot posterior predictive checks. We also use iqplot version 0.1.6 (Bois, 2020b) to visualize empirical cumulative distribution functions of our priors. Finally, other software we use in our analysis includes Holoviews version 1.14.5 (Rudiger et al., 2021), Bokeh version 2.3.3(Brendan Collins, 2020), Pandas version 1.3.1(Reback et al., 2021), SciPy version 1.6.2 (Virtanen et al., 2021), and NumPy version 1.20.3 (Harris et al., 2020).

Figure S10. C_3H_8 posterior samples for the conditional parameter and the hyperparameter during ATom 2 winter 2017. Top: 4x5. Middle: 2x2.5. Bottom: 0.5x0.625.

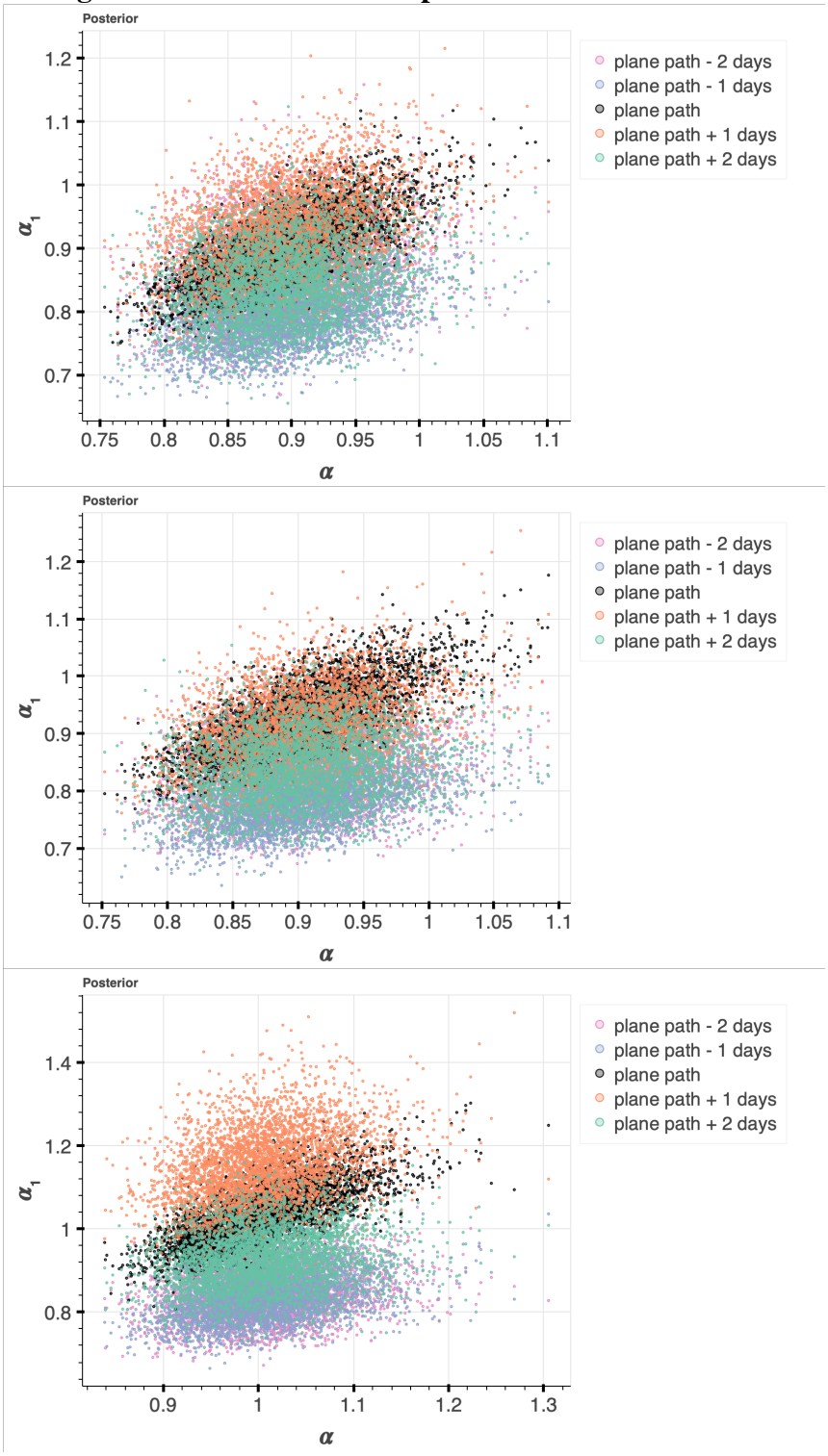

Figure S11. C_2H_6 posterior samples for the conditional parameter and the hyperparameter during ATom 2 winter 2017. Top: 4x5. Middle: 2x2.5. Bottom: 0.5x0.625.

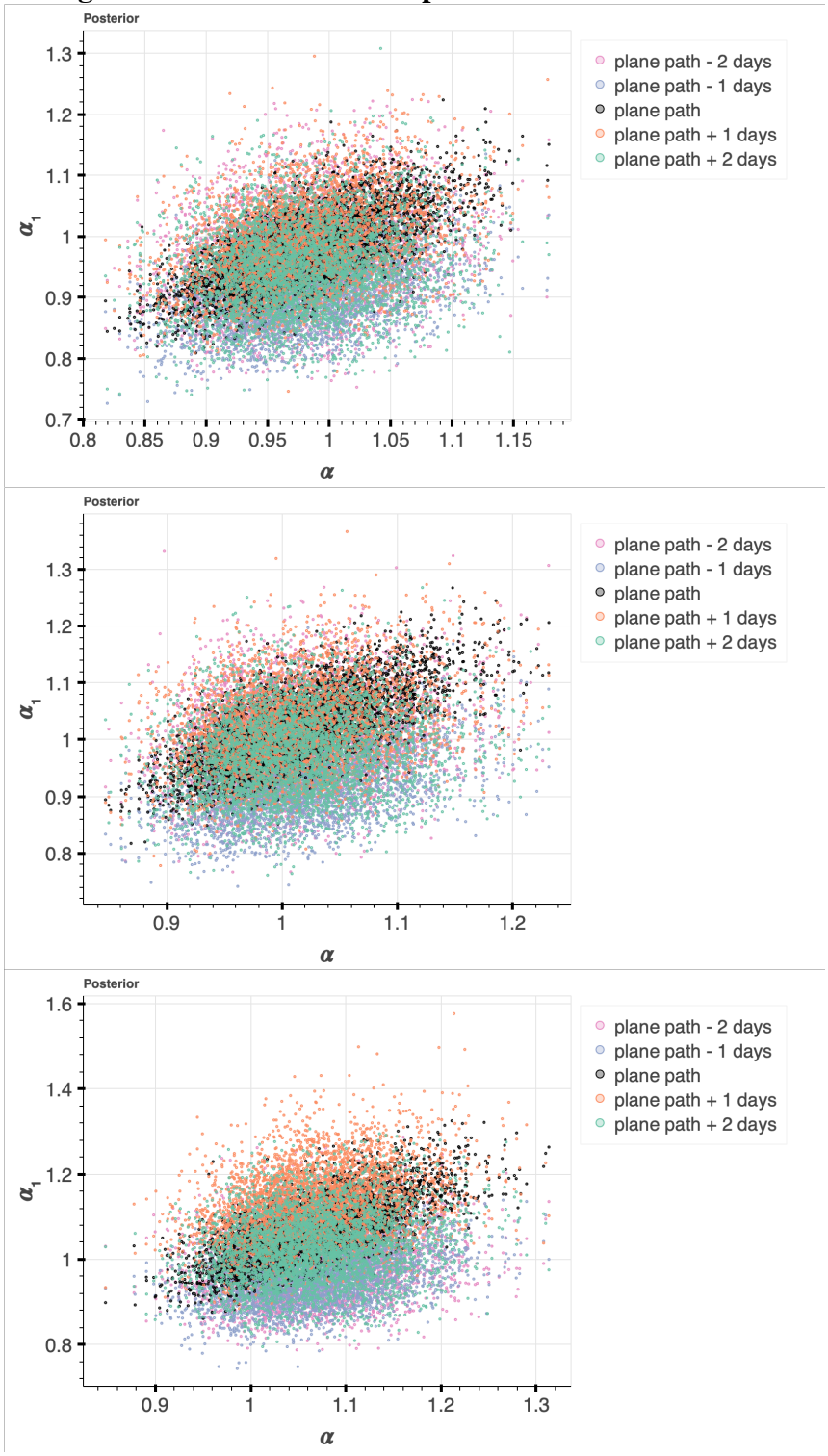

As in Tribby et al., (2022), we conduct posterior predictive checks, which involve drawing parameter values out of the posterior, using those parameters in the likelihood to generate a pseudo dataset, and continue repeating. This allows us to see whether the Bayesian model reproduces the observed data. Below, we show all posterior predictive checks for ATom2 Atlantic aircraft campaign. The majority of the measured data fell into the 30th and 50th percentile of the simulated Bayesian model data.

Figure S12. Posterior predictive check of C_3H_8 using ATom data. Left: 4x5. Middle: 2x2.5. Right: 0.5x0.625. Samples are during ATom 2 winter 2017. GCS represents GEOS-Chem simulations, interpolated to aircraft latitude, longitude, time, and potential temperature. Pseudo data are shown in blue with 30, 50, 70, 99th percentiles. Please see Table 1 in main text for value used to scale GCS data, determined via Bayesian inference.

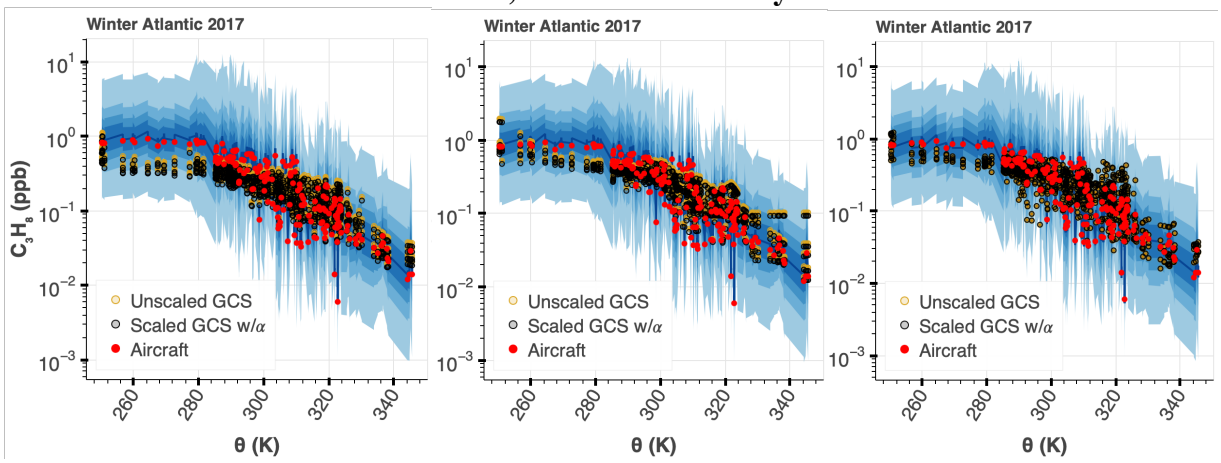

Figure S13. Posterior predictive check of C_2H_6 using ATom data. Left: 4x5. Middle: 2x2.5. Right: 0.5x0.625. Samples are during ATom 2 winter 2017. GCS represents GEOS-Chem simulations, interpolated to aircraft latitude, longitude, time, and potential temperature. Pseudo data are shown in blue with 30, 50, 70, 99th percentiles. Please see Table 1 in main text for value used to scale GCS data, determined via Bayesian inference.

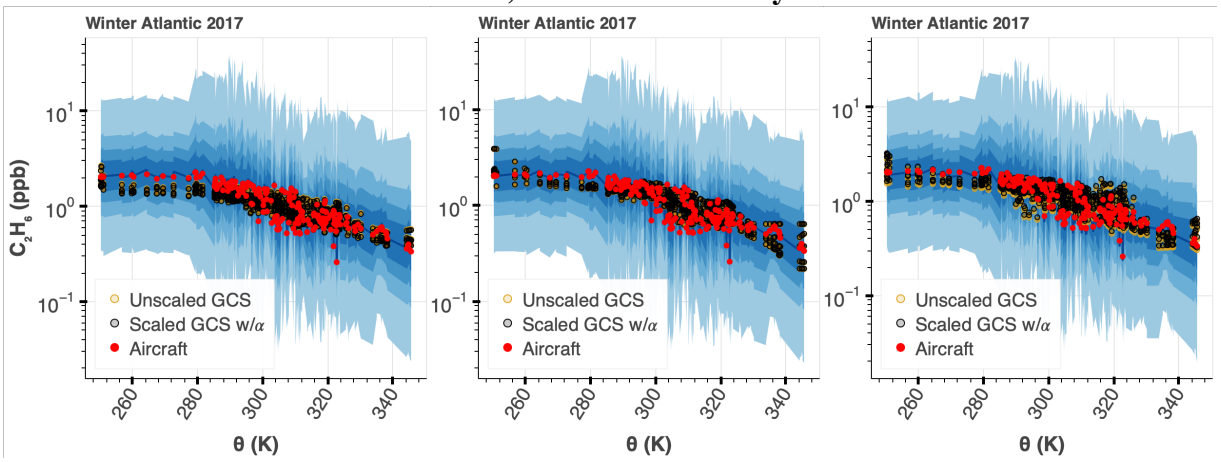

References

Bois, J.: justinbois/bebi103: 0.1.0, https://doi.org/10.22002/D1.1615, 2020a.

Bois, J. S.: justinbois/iqplot: 0.1.6, https://doi.org/10.22002/D1.1614, 2020b.

Brendan Collins, B. V. D. V.: Bokeh: Essential Open Source Tools for Science, https://doi.org/10.5281/ZENODO.4317717, 2020.

Harris, C. R., Millman, K. J., van der Walt, S. J., Gommers, R., Virtanen, P., Cournapeau, D., Wieser, E., Taylor, J., Berg, S., Smith, N. J., Kern, R., Picus, M., Hoyer, S., van Kerkwijk, M. H., Brett, M., Haldane, A., del Río, J. F., Wiebe, M., Peterson, P., Gérard-Marchant, P., Sheppard, K., Reddy, T., Weckesser, W., Abbasi, H., Gohlke, C., and Oliphant, T. E.: Array programming with NumPy, Nature, 585, 357–362, https://doi.org/10.1038/s41586-020-2649-2, 2020.

Kumar, R., Carroll, C., Hartikainen, A., and Martin, O.: ArviZ a unified library for exploratory analysis of Bayesian models in Python, J. Open Source Softw., 4, 1143, https://doi.org/10.21105/joss.01143, 2019.

Reback, J., Jbrockmendel, McKinney, W., Van Den Bossche, J., Augspurger, T., Cloud, P., Hawkins, S., Gfyoung, Sinhrks, Roeschke, M., Klein, A., Terji Petersen, Tratner, J., She, C., Ayd, W., Hoefler, P., Naveh, S., Garcia, M., Schendel, J., Hayden, A., Saxton, D., Shadrach, R., Gorelli, M. E., Jancauskas, V., Fangchen Li, Attack68, McMaster, A., Battiston, P., Skipper Seabold, and Kaiqi Dong: pandas-dev/pandas: Pandas 1.3.1, , https://doi.org/10.5281/ZENODO.5136416, 2021.

Rudiger, P., Stevens, J.-L., Bednar, J. A., Nijholt, B., Mease, J., Andrew, B, C., Randelhoff, A., Tenner, V., Maxalbert, Kaiser, M., Ea42gh, Stonebig, Hoxbro, Samuels, J., Pevey, K., LB, F., Tolmie, A., Stephan, D., Bois, J., Lowe, S., Bampton, J., Henriqueribeiro, Ruoyu0088, Lustig, I., Klein, A., Van De Ven, B., Raillard, D., Signell, J., and Talirz, L.: holoviz/holoviews: Version 1.14.5, , https://doi.org/10.5281/ZENODO.5114034, 2021.

Stan Dev Team: CmdStanPy (0.9.76), 2021a, https://pypi.org/project/cmdstanpy.

Stan Development Team: Stan Modeling Language Users Guide and Reference Manual (2.27), 2021b, https://mc-stan.org.

Talts, S., Betancourt, M., Simpson, D., Vehtari, A., and Gelman, A.: Validating Bayesian Inference Algorithms with Simulation-Based Calibration, ArXiv180406788 Stat, 2020.

Virtanen, P., Gommers, R., Burovski, E., Oliphant, T. E., Weckesser, W., Cournapeau, D., Alexbrc, Reddy, T., Peterson, P., Haberland, M., Wilson, J., Nelson, A., Endolith, Mayorov, N., Walt, S. V. D., Ilhan Polat, Laxalde, D., Brett, M., Larson, E., Millman, J., Lars, Mulbregt, P. V., Eric-Jones, CJ Carey, Moore, E., Kern, R., Peterbell10, Leslie, T., Perktold, J., and Striega, K.: scipy/scipy: SciPy 1.6.2, , https://doi.org/10.5281/ZENODO.4635380, 2021.